Neuron, Volume *108*

Supplemental Information

Precise Holographic Manipulation of Olfactory Circuits Reveals Coding Features Determining Perceptual Detection

Jonathan V. Gill, Gilad M. Lerman, Hetince Zhao, Benjamin J. Stetler, Dmitry Rinberg, and Shy Shoham

Supplemental Information

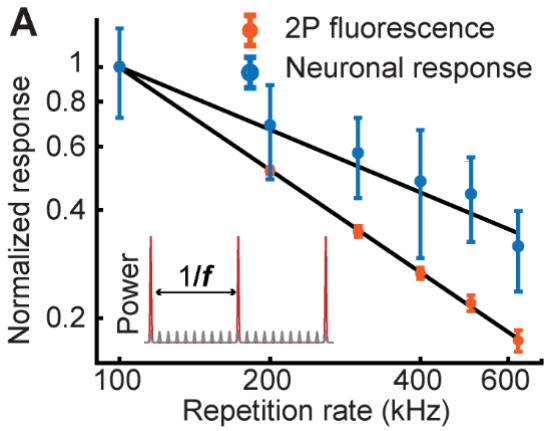

Figure S1. Characterization of 2P excitation dependence on repetition rate. (related to Figure 1) Evoked 2P fluorescence signal measured using fluorescein, and neuronal GCaMP6s responses as a function of the laser's repetition rate for a constant average power (mean ΔF/F ± SEM, n = 10 cells, 1 WT mouse, 30 stimulations per rep. rate). The data is normalized to the mean response value at the lowest repetition rate. Inset shows a schematic of the laser pulses for high and low repetition rates.

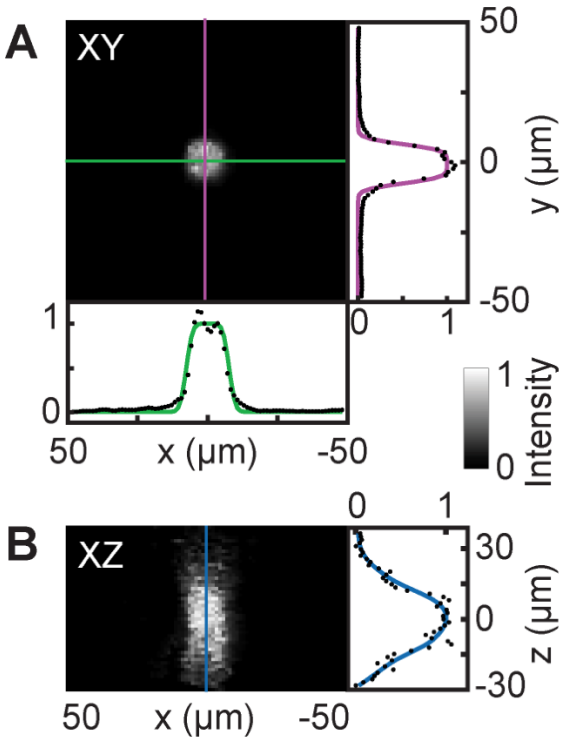

Figure S2. Photostimulation point spread function. (related to Figure 1) **A-B.** Light patches generated using the weighted Gerchberg-Saxton algorithm (Gerchberg and Saxton, 1972; Golan et al., 2009) were characterized using a widefield microscope. A thin (<5 μm) fluorescein layer was illuminated with a light patch and the 2P excited fluorescence signal was projected onto a CMOS camera. **A.** Normalized fluorescence intensity in the (*x,y*) plane at the focus (*z* = 0). The photostimulation point spread function measured 13 μm and 12.8 μm full width at half maximum (FWHM) in the *x* and *y* dimensions. A top-hat function convolved with a Gaussian kernel was fit to the data for visualization. **B.** Normalized fluorescence intensity in the (*x,z*) plane (*y* = 0). The photostimulation point spread function measured 24.6 μm FWHM in the z dimension. Fluorescence values were fit with a cubic smoothing spline for visualization.

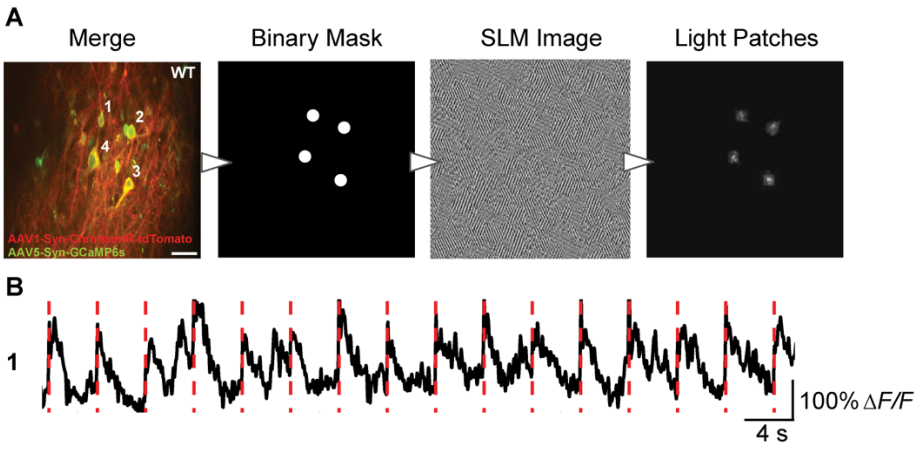

Figure S3. Holographically targeting multiple neurons with light patches. (related to Figure 1) **A**. Illustration of workflow for holographically targeting light patches to multiple neurons. Scale bar, 30 µm**. B**. Example trial-by-trial calcium response to photostimulation for one neuron (4 targeted neurons, 50 ms photostimulation, 16 trials, 0.1 mW/µm^2, n = 1 WT mouse).

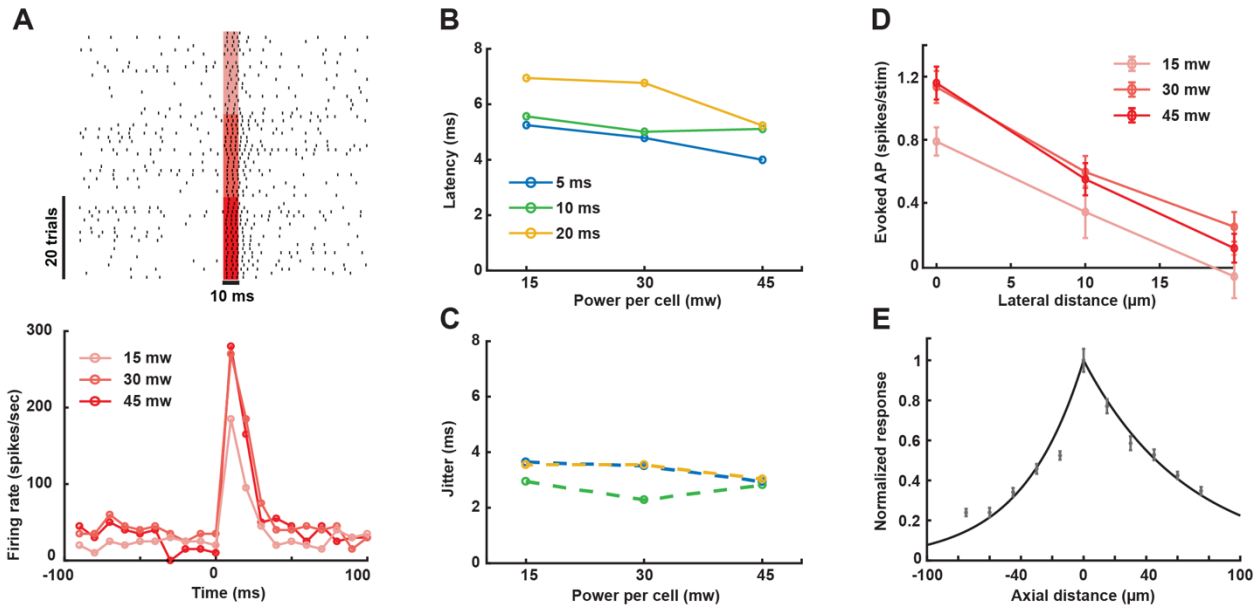

Figure S4. Electrophysiological characterization of photostimulation. (related to Figure 1) **A.** Example raster plots (top) and correspondent peristimulus time histograms (PSTHs) (bottom) for different stimulation powers, (red shading, photostimulation on; n = 1 cell, 1 WT mouse, 20 trials per condition). **B-C.** The average latency (**B**) and jitter (**C**) of evoked spikes as a function of power per cell for different stimulation durations. The latency is defined as the time from photostimulation onset to the first spike within a 20 ms window, and jitter is defined as the average of the standard deviation of the latency across trials and cells (n = 5 cells, 5 WT mice). **D-E.** The efficiency of photostimulation when moving the light patch away from the cell's soma laterally (**D,** mean ± SEM, n = 4 cells, 4 WT mice) and along the z-axis (**E,** mean ± SEM, n = 9 cells, 3 WT mice, 30 mW/patch, 0.19 mW/µm^2).

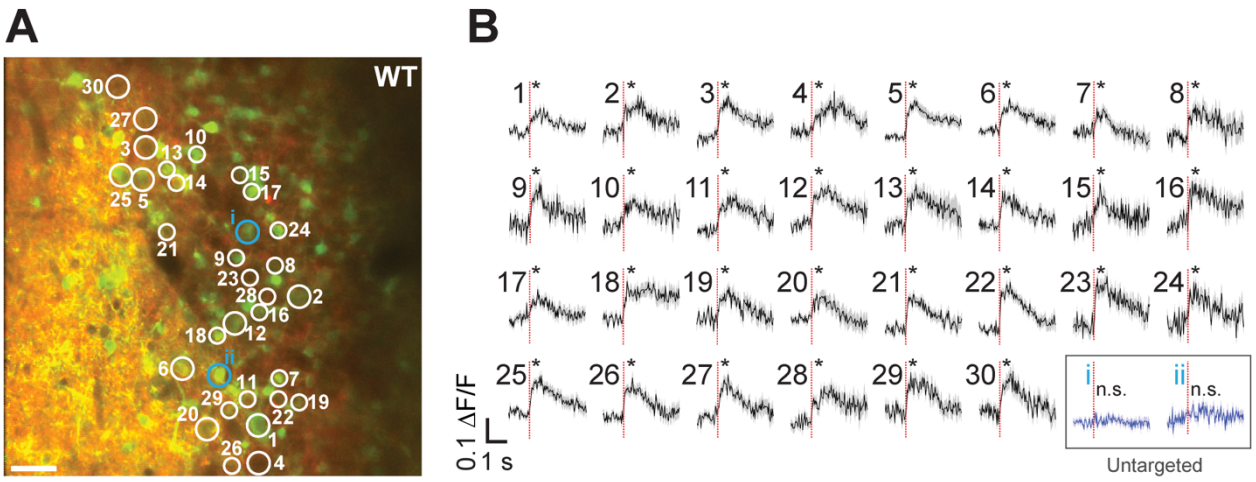

Figure S5. All-optical control of 30 neurons. (related to Figure 1) **A.** Thirty neurons were targeted for simultaneous 2P photostimulation (white circles) and 2P imaging (scale bar, 40 µm). **B.** Average GCaMP6s calcium response to photostimulation (red dashed line – stimulation onset) for 30 targeted neurons (black) and 2 example non-targeted neurons (blue) (mean ΔF/F ± SEM, *p<0.05, two-sample t-test, 30 trials, 10 ms stimulation duration, 18 mW/patch, 0.1 mW/µm^2, *n* = 1 WT mouse).

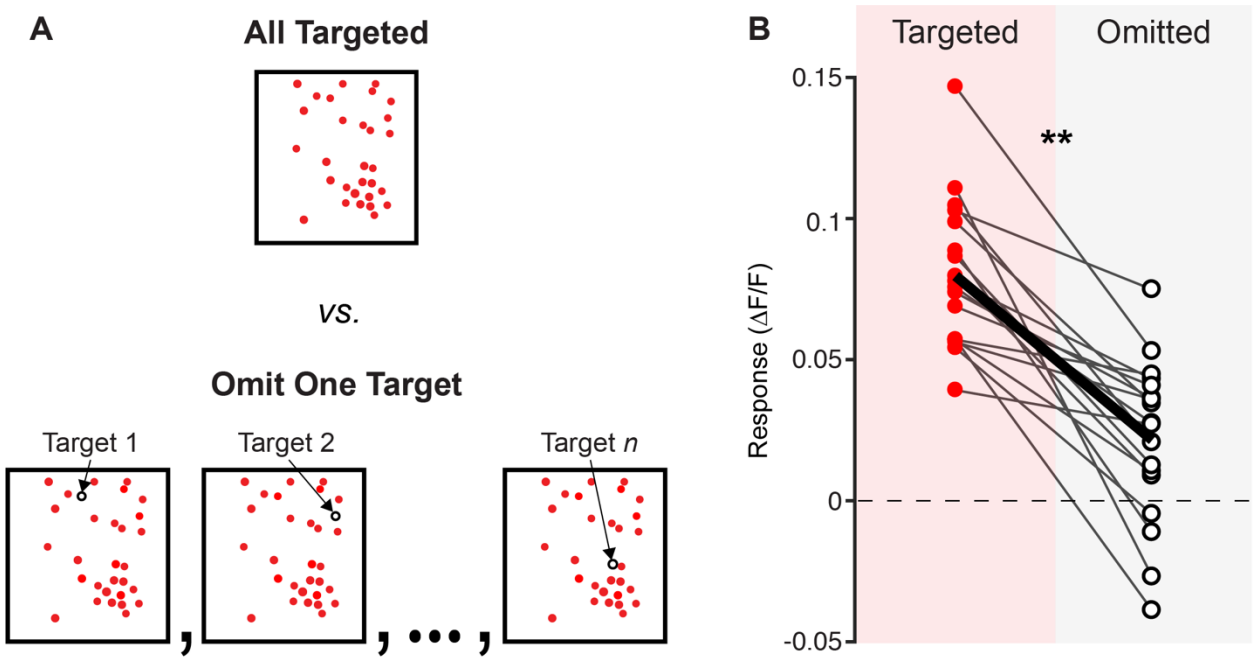

Figure S6. Characterizing response in omitted photostimulation targets. (related to Figure 1) **A.** Schematic of the omit-one-target experiment. Top. Pattern of spots targeting many neurons simultaneously. Bottom. Omit one target condition in which one of the spots is removed from the stimulation pattern. All spots are individually dropped, and the holograms are randomly presented to the mouse along with the all targeted hologram. **B**. Average response to 10 ms photostimulation. The average response per cell when it was targeted vs. when it was omitted with all other cells targeted. (**p<0.001, two-sample t-test, Targeted: 0.08 ± 0.006, vs. Omitted: 0.02 ± 0.007, mean ΔF/F ± SEM, 28 targeted cells (19 responsive), n = 2 WT mice, 30 photostimulations per datapoint, 10 ms duration, 20 mW/patch, 0.125 mW/μm^2).

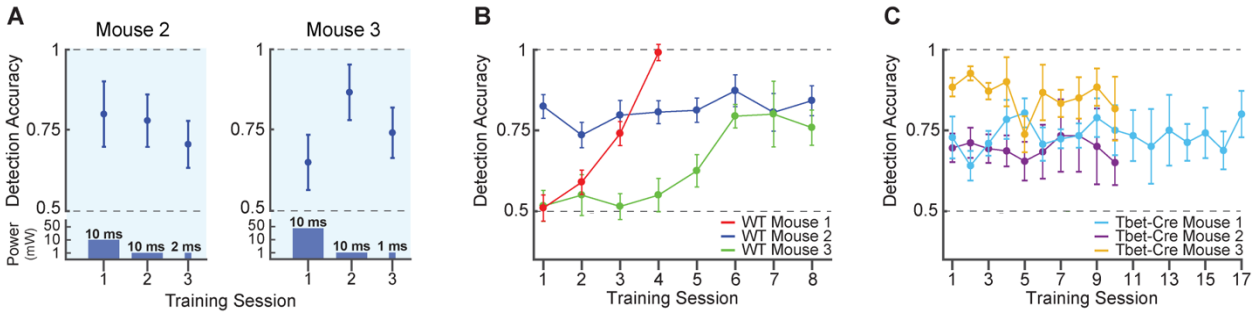

Figure S7. Photostimulation detection training. (related to Figure 2) **A**. Performance for 1-photon photostimulation detection training for individual mice. 1-photon photostimulation energy was decreased from session to session (mean ± 95% confidence intervals). Power and duration of 1-photon stimulation is schematized at the bottom of the graph. **B**. Performance for 2P photostimulation detection of the same 30 neurons (mitral and granule cells) across sessions (mean ± 95% confidence intervals, $n = 3$ WT mice, 0.1-0.125 mW/µm^2). All mice reached a performance >75% correct within 7 sessions. **C**. Detection accuracy of 2P photostimulation targeting the same mitral cells across sessions in Tbet-Cre mice (mean ± 95% confidence intervals, $n = 3$ Tbet-Cre mice, 0.1-0.15 mW/µm^2). The number of mitral cells targeted was 17, 11 and 27 in mouse 1, 2 and 3, respectively.

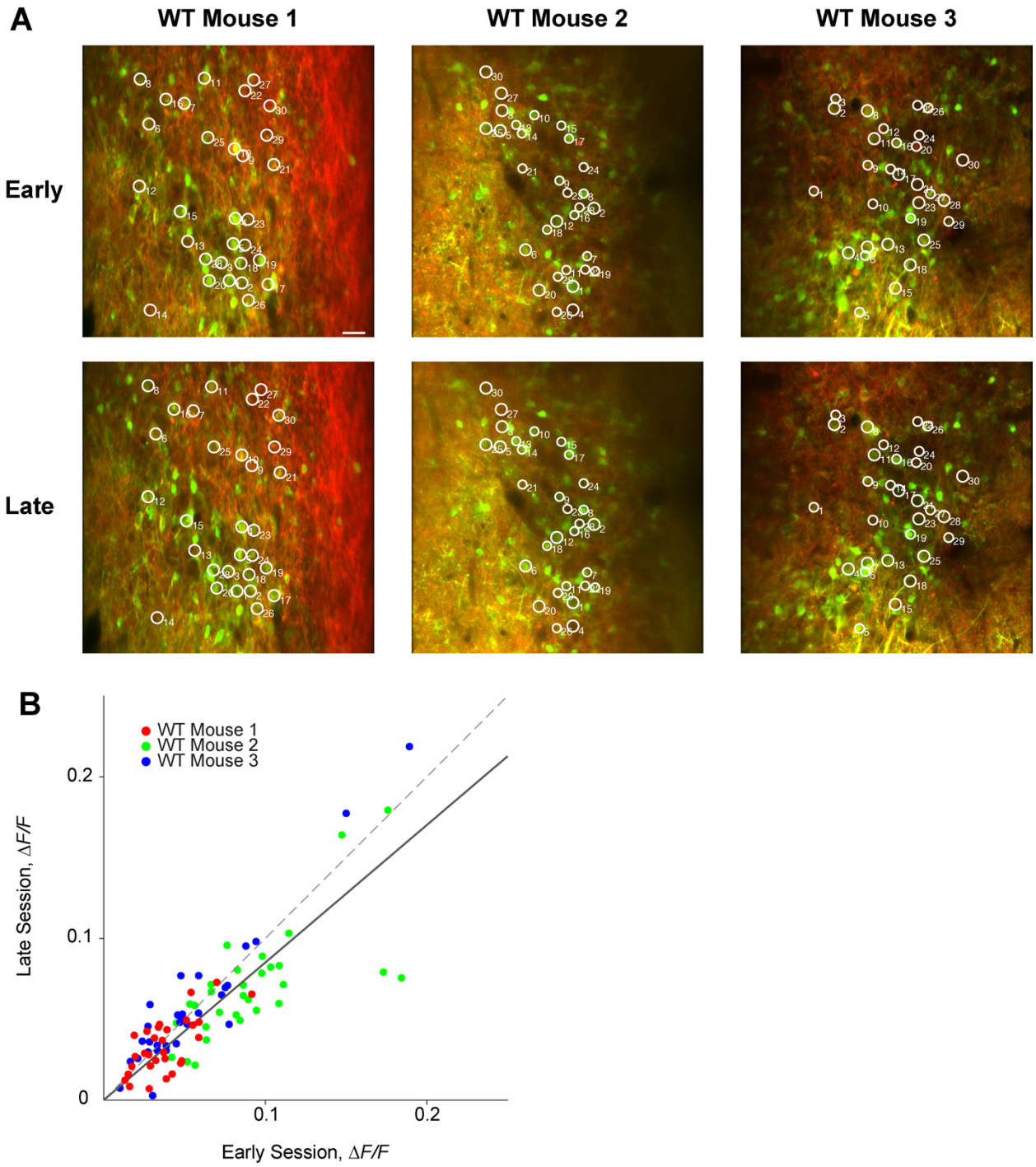

Figure S8. Stability of neuronal targeting and responses across sessions. (related to Figure 2) **A**. Example fields of view and targeted neurons (white circles) imaged early in training (upper) or late in training (lower) for three WT mice. ChrimsonR-tdTomato expression is shown in red, GCaMP6s expression in green. Scalebar = 30 µm. **B**. Mean response to photostimulation was highly correlated across sessions (30 trials per session, 10 ms stimulation duration, $n = 3$ WT mice, 0.1 mW/µm^2). Data points represent $\Delta F/F$ values averaged over 330 ms following stimulation. Dashed line is the unity line and the solid line is the linear fit (slope = 0.85).

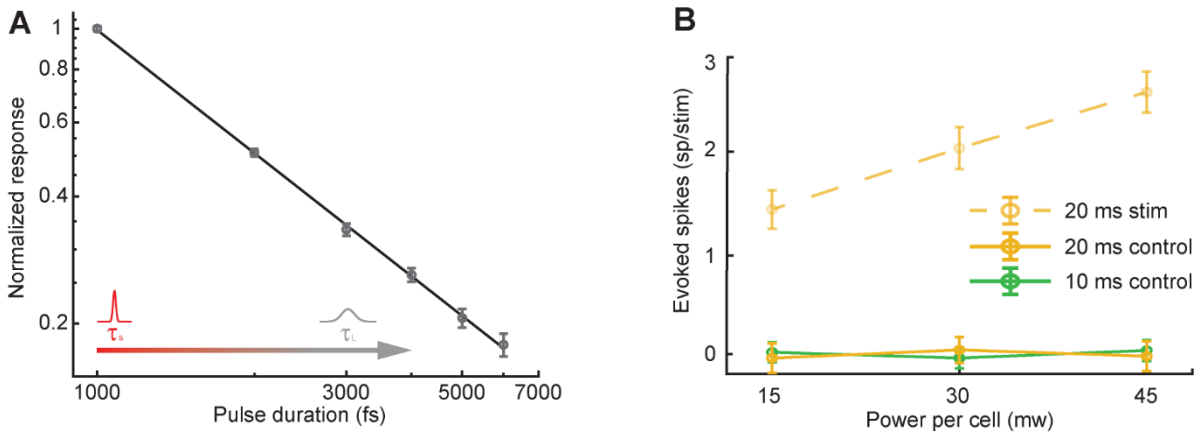

Figure S9. Pulse duration effects characterization. (related to Figure 3) **A**. Normalized excited 2P fluorescence in fluorescein as a function of pulse width (mean ΔF/F ± SEM). **B.** Average number of spikes evoked by long-pulse (solid line) and short pulse (dashed line) photostimulations. There was no significant change in the number of evoked spikes compared to baseline (mean ± SEM, $p = 0.99$, Wilcoxon rank-sum test, $n = 4$ cells, 4 WT mice).

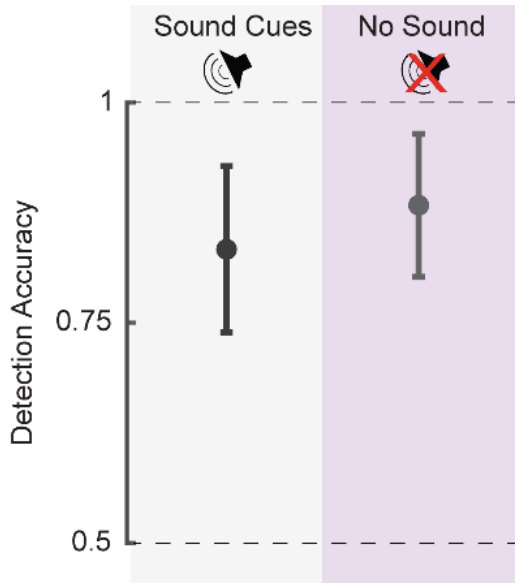

Figure S10. Detection in the absence of sound cues. (related to Figure 3) Detection accuracy in two sequential blocks of trials where sound cues were either present or omitted (error bars = ± 95% confidence intervals, $p = 0.6$, Fisher's exact test, 27 targeted mitral cells, 60 trials/data point, 20 mW/patch, 0.125 mW/μm^2, $n = 1$ Tbet-cre mouse).

Single-Cell photostimulation response predictions

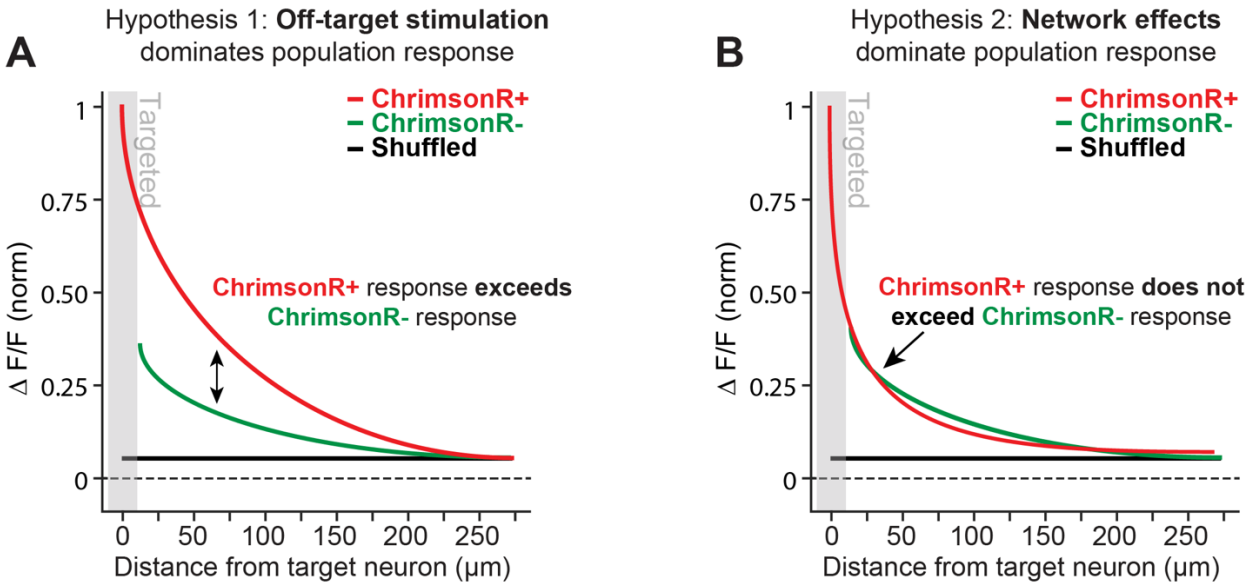

Multiple-Cell photostimulation response predictions

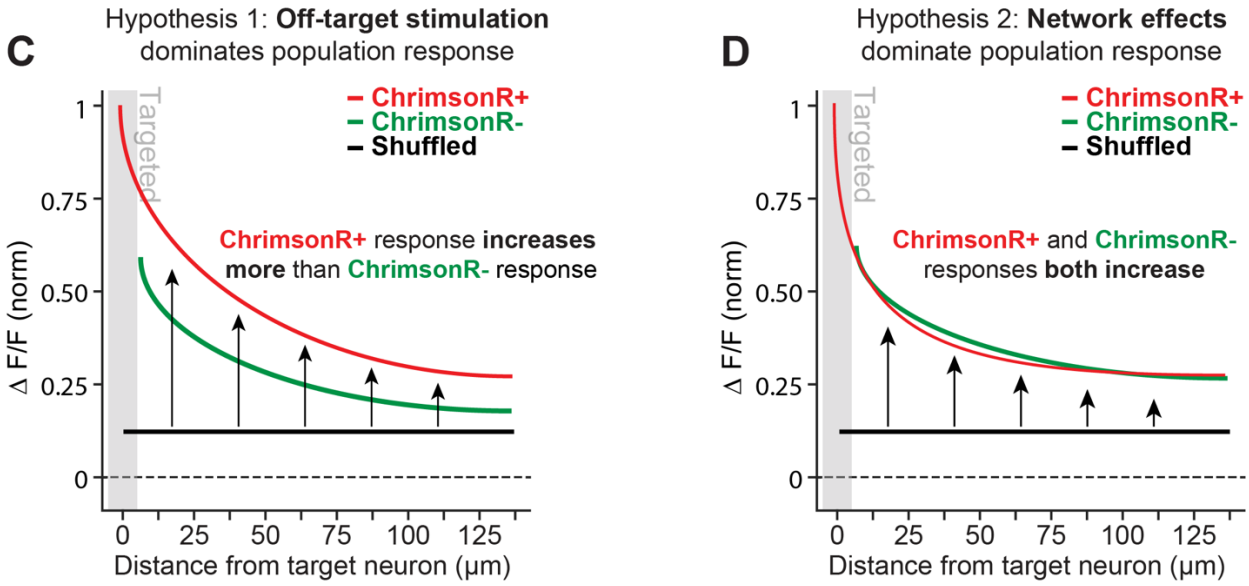

Figure S11. Expected effects on population responses as a function of eccentricity from targeted neurons. (related to Figure 4) **A-D.** Schematic of possible response profiles for opsin-positive/negative (ChrimsonR+, ChrimsonR-) neurons in Tbet-cre mice as a function of eccentricity from photostimulation targeted neurons under different degrees of off-target (accidental) or network (synaptically) driven activations. Red and green curves represent the mean response across cell types (ChrimsonR+, ChrimsonR-) at different radial eccentricities from targeted neurons. Shuffled curves represent the mean response of both ChrimsonR+ and ChrimsonR- neurons to randomly selected intervals during blocks of photostimulation trials. **A.** Expected outcome if photostimulation activates neighboring ChrimsonR+ neurons due to off-target photostimulation: ChrimsonR+ responses will exceed the of ChrimsonR- responses reflecting inadvertent stimulation of nearby Chrimson+ neurons. **B.** Expected outcome if single-cell photostimulation led to responses of nearby neurons due to network effects: ChrimsonR+ responses lack (the inadvertent) excess excitation and would not exceed the responses of ChrimsonR- neurons. **C-D.** During multiple-cell photostimulation, network mediated modulation of nearby neurons is expected to increase relative to single-cell photostimulation, leading to an upward shift in population response across eccentricities. **C.** If off-target photostimulation effects increase with an increase in the number of targeted neurons, ChrimsonR+ responses should increase more than ChrimsonR- responses. **D.** If network effects increase with the number of targeted neurons, but not off-target photostimulation, ChrimsonR+ and ChrimsonR- neurons should both similarly increase their responses across eccentricities.

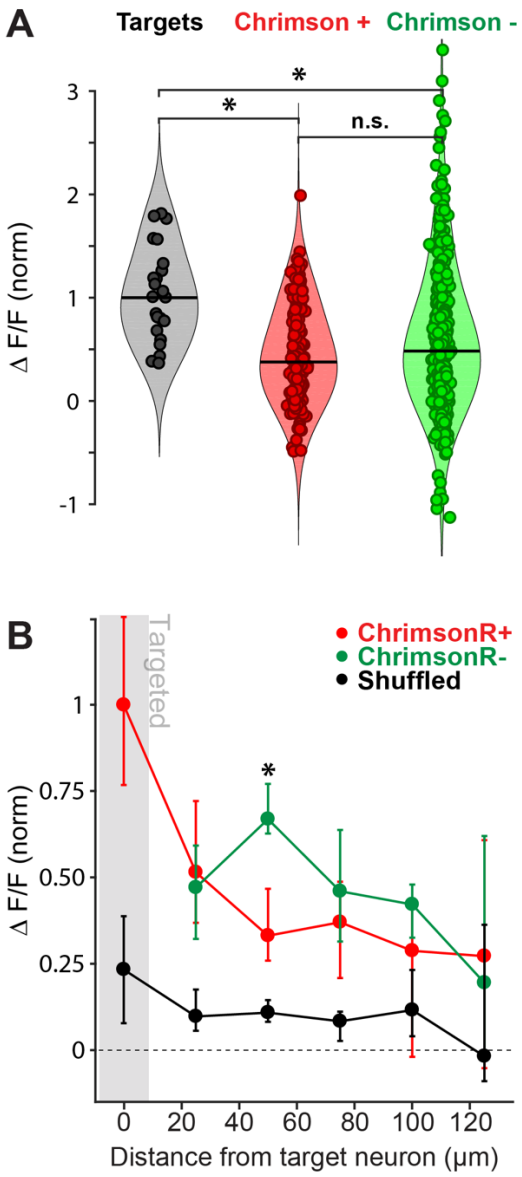

Figure S12. Distribution of responses during photostimulation of multiple targets. (related to Figure 4) **A.** Distribution of average responses in targeted mitral cells and untargeted opsin-positive (ChrimsonR+) and opsin-negative (ChrimsonR-) neurons following photostimulation of multiple neurons (black bars = median, *p<0.05, Wilcoxon rank-sum test, 11-27 MCs targeted simultaneously, 183 Chrimson+ and 369 Chrimson- neurons, n = 3 Tbet-cre mice, 20 mW/patch, 0.125 mW/μm^2, data normalized to median target response). **B.** Response as a function of opsin expression and eccentricity from targeted mitral cells (median ± 95% confidence intervals, *p < 0.05, ChrimsonR+ vs. ChrimsonR-, Wilcoxon rank-sum test, Holm-Bonferroni corrected for multiple comparisons, n = 3 Tbet-cre mice, 20 mW/patch, 0.125 mW/μm^2, data normalized to median target response). Shuffled data corresponds to the distribution of binned responses of the same neurons with stimulation times randomly chosen (see STAR Methods).

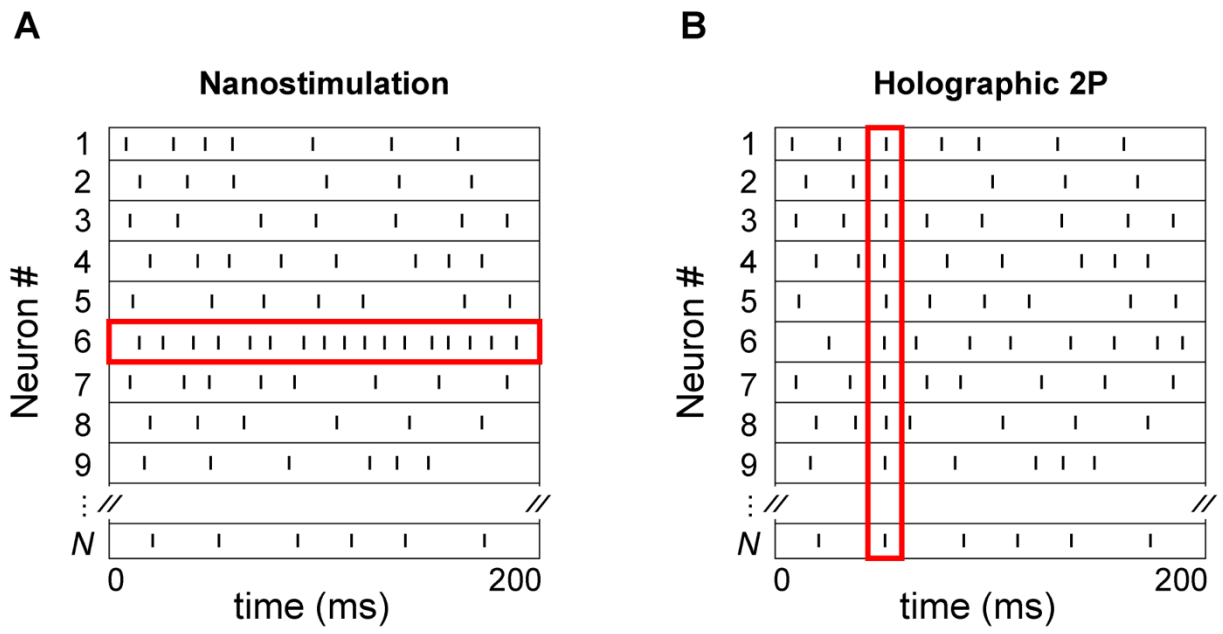

Figure S13. Experimental paradigms exploring different modes of spike detectability. (related to Figure 5) **A-B.** Nanostimulation and holographic 2P photostimulation address different and complementary coding strategies. **A.** Nanostimulation explores detection sensitivity to increases in the spike rate of individual neurons over 100s of milliseconds **B.** Holographic 2P photostimulation explores detection sensitivity to spikes coordinated across individually selected neurons on a timescale of <10 ms.